Electronic Supplementary Material (ESI) for ChemComm.

Supporting Information

Mixed Noble Metal-Oxo Clusters: Platinum(IV)-Gold(III) Oxoanion $[Pt^{IV}_2Au^{III}_3O_6((CH_3)_2AsO_2)_6]^-$

Jiayao Zhang,[a] Saurav Bhattacharya,[a,b] Anja B. Müller,[a] Levente Kiss,[c] Cristian Silvestru,[c] Nikolai Kuhnert,[a] and Ulrich Kortz*[a]

a. School of Science, Constructor University (formerly Jacobs University), Campus Ring 1, 28759 Bremen (Germany), E-mail: ukortz@constructor.university, u.kortz@jacobs-university.de, Web http://ukortz.user.jacobs-university.de/

b. Department of Chemistry, BITS Pilani K. K. Birla Goa Campus, 403726 Goa, India

c. Department of Chemistry, Supramolecular Organic and Organometallic Chemistry Centre (SOOMCC), Faculty of Chemistry and Chemical Engineering, Babes-Bolyai University, 400028 Cluj-Napoca, Romania

1. Experimental details

General methods and materials. The reagents were used as purchased without further purification. Hydrogen tetrachloroaurate(III) hydrate was a purum grade with ~50% Au basis (Sigma-Aldrich). Hydrogen hexahydroxyplatinate(IV) was 99.9% trace metal basis (Sigma-Aldrich). Elemental analyses were performed by Technische Universität Hamburg (TUHH, Zentrallabor Chemische Analytik, Hamburg, Germany) and Analytische Laboratorien (Lindlar, Germany). The Na analysis was performed in house by atomic absorption (AA) spectroscopy using a Varian SpectrAA 220 AA spectrometer. The crystal water content was determined by thermogravimetric analysis (TGA) on a TA Instruments Q600 device. The TGA curve of freshly prepared **Na-1** indicated an initial weight loss of ~5%, which corresponds to the loss of the lattice water molecules as based on elemental analysis (calculated ~5%). The TGA curve of freshly prepared **K-1** indicated an initial weight loss of ~12%, which corresponds to the loss of the lattice water molecules as based on elemental analysis (calculated ~12.8%). Infrared spectra were recorded on KBr disks using a Nicolet-Avatar 370 spectrometer. The NMR spectra were recorded on a 400 MHz JEOL-ECA instrument at room temperature using 5-mm tubes. The resonance frequency for ^{195}Pt NMR was 85.94 MHz and the chemical shifts are reported with respect to 1M Na_2PtCl_6 in H_2O/D_2O as the 0 ppm reference. The ^{195}Pt NMR spectra were acquired the simple zg pulse sequence, using an acquisition time of 0.3028 sec, and a relaxation delay of 1 sec. High-resolution ESI-MS spectra were recorded using a Bruker Daltonics micrOTOF Focus instrument employing both negative and positive electrospray ionization modes. MicrOTOF Focus mass spectrometer (Bruker Daltonics) was fitted with an ESI source and external calibration was achieved with 10 mL of 0.1M sodium formate solution. The instrument ion source and tubing were rinsed with methanol. The calibration was carried out using the enhanced quadratic calibration mode. All ESI-MS measurements were performed in both negative and positive ion modes. The samples were measured as direct infusions using 0.001M aqueous methanol (50:50) solutions at a flow rate of 180 μL/min. The spectral simulation was carried out using Data Analysis 4.1 (Bruker Daltonics, Bremen). Powder X-ray diffraction data were acquired on a Rigaku Miniflex 600 (Rigaku Corporation, Tokyo, Japan) using a primary beam Cu Kα radiation (λ = 1.541838 Å) at 40 kV and 15 mA. The instrument scanning 2θ range was from 5 to 50º in steps of 0.02º, with a scan speed of 5 º min^{-1}.

Synthesis. $Na[Pt^{IV}_2Au^{III}_3O_6(AsO_2(CH_3)_2)_6]\cdot NaCl\cdot NaNO_3\cdot 6H_2O$ (**Na-1**): $H[AuCl_4]$ (0.061 g, 0.18 mmol) was dissolved in 1.5 mL aqueous sodium cacodylate buffer (2 M, adjust pH to 7 by adding 68% HNO_3), leading to an orange solution. Then $H_2Pt(OH)_6$ (0.036 g, 0.12 mmol) was dissolved in 0.4 mL 1M NaOH solution, and added to the resulting orange solution while heating at 80 °C. During the dropwise addition of $H_2Pt(OH)_6$, the color of the reaction mixture changed from orange to orange-red. The obtained solution was stirred at 80 °C for 30 min. Slow evaporation of the filtrate at room temperature in an open vial resulted in yellow hexagonal crystals within 2 days. The obtained crystals **Na-1** were collected after 5 days by filtration and air dried for 2 days. Yield: 0.085 g (68% based on Au). Upon rehydration, **Na-1** can be fully transformed to the crystalline phase in the mother liqour **Na-1a** (see main text for details). Polyanion **1** can also be synthesized using the reagents in stoichiometric ratio in water (instead of cacodylate buffer), but the yield was only 35%. FT-IR (KBr, cm^{-1}): 3529–3143 (s) [υ(O–H) of H_2O], 3000–2800 (w) [υ(C–H) of methyl groups of cacodylate], 1597 (m) [H_2O bending fundamental mode δ], 1381 (m) [δ(C–H) of the methyl groups of cacodylate], 913 (w) [$\delta_{out\text{-}of\text{-}plane}$(O–H)], 803 (s) [υ(Au–O)], 679–646 (w) [υ(Pt–O)], 566–452 (m) [υ(As–C)]. Elemental analysis (%) calcd for **Na-1**: Au 27.18, Pt 17.95, As 20.68, Na 3.17,Cl 1.63, N 0.64, C 6.63, H 2.23; found: Au 26.80, Pt 18.90, As 20.80, Na 3.35, Cl 2.60, N 0.73, C 6.65, H 2.18. $K[Pt^{IV}_2Au^{III}_3O_6(AsO_2(CH_3)_2)_6]\cdot KCl\cdot KAsO_2(CH_3)_2\cdot 18H_2O$ (**K-1**): $H[AuCl_4]$ (0.061 g, 0.18 mmol) was dissolved in 1.5 mL aqueous cacodylic acid buffer (2 M, adjust pH to 7 by adding solid KOH), leading to an orange solution. Then $H_2Pt(OH)_6$ (0.036 g, 0.12 mmol) was dissolved in 0.4 mL 1 M KOH solution, and added to the orange solution while heating at 80 °C. During the dropwise addition of $H_2Pt(OH)_6$, the color of the reaction mixture changed from orange to orange-red. The obtained solution was stirred at 80 °C for 30 min. Slow evaporation of the filtrate at room temperature in an open vial resulted in yellow rod-shaped crystals within 1 month. The obtained crystals were collected by filtration and dried in air. Yield: 0.068 g (46% based on Au). FT-IR (KBr pellet, cm^{-1}): 3407 (s) [υ(O–H) of H_2O], 3019–2924 (w) [υ(C–H) of methyl groups of cacodylate], 1668-1643 (m) [H_2O bending fundamental mode δ], 1411 (m) [δ(C–H) of the methyl groups of cacodylate], 915 (w) [$\delta_{out\text{-}of\text{-}plane}$(O–H)], 810 (s) [υ(Au–O)], 702–648 (w) [υ(Pt–O)], 523 (m) [υ(As–C)]. Elemental analysis (%) calcd for **K-1**: Au 23.51, Pt 15.53, As 20.87, K 4.67, C 6.69, H 2.13; found: Au 23.50, Pt 15.70, As 20.60, K 4.37, C 6.62, H 2.60.

2. X-ray crystallography. Crystal data for **Na-1**, **Na-1a** and **K-1** were collected at 100 K on a Bruker D8 APEX II CCD single-crystal diffractometer equipped with kappa geometry (graphite monochromator, $\lambda_{Mo\ K\alpha}$ = 0.71073 Å) by using the APEX III software package.[1] The crystals were mounted in a Hampton cryoloop with paratone-N oil. Multi-scan absorption corrections were applied using the SADABS program.[2] The structures were solved by direct methods with the aid of successive difference Fourier maps, and were refined against all data using the APEX III software in conjunction with SHELXL-2014.[3] The H atoms of the cacodylate methyl groups were placed in calculated positions and refined using a riding model and the remaining non-hydrogen atoms were refined with anisotropic displacement parameters. All atoms were refined anisotropically, except for some oxygen atoms of crystal waters. Refinements were conducted by full-matrix least squares against $|F|$ using all data. Images of the crystal structures were generated by Diamond, version 3.2 (copyright Crystal Impact GbR). Some of the lattice water molecules were heavily disordered and thus the disagreeable reflections were removed by the SQUEEZE command in PLATON.[4] The solvent masking was done using the SQUEEZE command of Platon, the results of which have been added to the CIF files in the section titled "SQUEEZE RESULTS". From the calculations, it can be seen that the solvent accessible void of the crystal structure **Na-1a** is ~739 Å^3, and the electron count in the solvent accessible void is ~291. Considering Z = 2, this roughly comes out to be around 14 H_2O molecules, which is larger as compared to what is observed from TGA analysis and elemental analysis (this air-dried material actually corresponds to the compound **Na-1**). This is typically due to the facile removal of the lattice water molecules (converting **Na-1a** to **Na-1**), which we have carefully studied using SXRD, PXRD and TGA. Similarly, for **K-1**, we observed a solvent accessible void of ~148 Å^3, and the electron count in the solvent accessible void to be ~90. Considering Z = 2, this roughly comes out to be around 5 H_2O molecules. If we add this to the 11 H_2O molecules already assigned from XRD, we get 16 lattice H_2O molecules, which is very close to what is observed from TGA analysis and elemental analysis (~18 lattice H_2O molecules). The crystallographic data for **Na-1**, **Na-1a** and **K-1** are summarized in Table S1. For **Na-1a**, two Au positions are disordered within the structure due to thermal motion, with partial occupancies of 47:3. For **K-1**, two As positions of free cacodylate ions are disordered within the structure due to thermal motion, with partial occupancies of 80:20. The disorder on the Au atom in **Na-1a** has been modelled by using the PART function and allowing for free refinement of the occupancies of the disordered atoms as well as their thermal parameters. This indicated a ~6% disorder

on the Au atom. Based on our observations from PXRD studies, we seem to form a mixture of two closely related crystalline phases differing in the amounts of lattice water molecules (**Na-1** and **Na-1a**). Even a slight exposure to air results in the removal of some of the lattice water molecules, which may lead to the observed disorder in the Au atoms as such a phase change appears to be facile. The cif files are provided free of charge by the Cambridge Crystallographic Data Centre (CCDC 2249169, 2221906, 2221907).

3. Bond valence sum calculations

The bond valence sum (BVS) calculations were performed on a program copyrighted by Chris Hormillosa & Sean Healy and distributed by I. D. Brown.[5] In **Na-1** and **Na-1a**, the BVS values for the independent gold atom are 2.911 and 2.592, and the values for the independent platinum atom are 3.798 and 4.348, respectively. The BVS values for different types of μ_2-bridging oxygens are presented in Table S4. These values show that these oxygens are not protonated and therefore polyanion **1** is a true gold(III)-platinum(IV) oxo species. In **K-1**, the BVS values for the three gold atoms range from 2.609 to 2.665, and the values for the two platinum atoms are 4.209 and 4.228, respectively, supporting the +3 oxidation state of gold and +4 oxidation state of platinum in polyanion **1**.

4. Light irradiation

We have also investigated the stability of solid **Na-1** under blue light (λ = 450-480 nm, blue LED lamp LED PAR30, E-27). The PXRD spectra revealed that the crystal structure maintains a high degree of crystallinity up to at least 4 h (Figure S13). Regarding solutions of **Na-1** in water upon irradiation with blue light, ^{1}H NMR revealed that the free cacodylate signal at 1.6 ppm gradually increased from the original 0% to 2, 3, 6, 14, 17 and 20% after 5, 15, 30, 60, 120 and 240 min, respectively (Figure S14). Without irradiation, ^{1}H NMR demonstrated that there is only a 2% decomposition of **Na-1** after 1 day (Figure S14).

References

[1] *APEX suite of crystallographic software*, *APEX 3*, *version 2015.5-2*, Bruker AXS Inc., Madison, Wisconsin, USA, **2015**.

[2] SAINT, Version 7.56a and SADABS Version 2008/1, Bruker AXS Inc., Madison, Wisconsin, USA, **2008**.

[3] G. M. Sheldrick "*SHELXL-2014*", University of Göttingen, Göttingen, Germany, **2014**.

[4] A. L. Spek, *PLATON*, *A Multipurpose Crystallographic Tool*, Utrecht University, Utrecht, The Netherlands, **2010**.

[5] I. D. Brown, D. Altermatt, *Acta Crystallogr.* **1985**, *B41*, 244-247.

Table S1. Crystal data and structure refinement parameters for **Na-1**, **Na-1a** and **K-1**.

Compound	**Na-1**	**Na-1a**	**K-1**
empirical formula	$Na_3Pt_2Au_3As_6C_{12}H_{48}O_{27}NCl$[a]	$Na_3Pt_2Au_3As_6C_{12}H_{36}O_{27}NCl$	$K_3Pt_2Au_3As_7C_{14}H_{78}O_{38}Cl$[a]
fw, g mol^{-1}	2173.51[a]	2161.44	2513.00[a]
crystal system	Hexagonal	Hexagonal	Triclinic
space group	$P\bar{6}$	$P6_3/m$	$P\bar{1}$
a(Å)	10.933(3)	10.9156(7)	13.5559(16)
b(Å)	10.933(3)	10.9156(7)	14.1105(16)
c(Å)	20.585(5)	26.8948(18)	16.6726(19)
α(º)	90	90	75.614(3)
β(º)	90	90	66.913(3)
γ(º)	120	120	85.534(3)
V (Å^3)	2130.9(12)	2775.2(4)	2841.1(6)
Z	1	2	2
Dc (g cm^{-3})	1.684	2.587	2.790
abs coeff, mm^{-1}	10.817	16.612	17.013
θ range for data collection, deg	3.667 to 24.850	3.719 to 26.382	2.970 to 25.790
completeness to Θ_{max}	99.2%	99.5%	99.6%
index ranges	-12 =< h =< 12,	-13 =< h =< 12,	-16 =< h =< 16,
	-12 =< k =< 12,	-13 =< k =< 13,	-17 =< k =< 17,
	-20 =< l =< 24	-33 =< l =< 33	-18 =< l =< 20
reflns collected	22878	36290	33904
indep reflns	2531	1944	10846
R(int)	0.1073	0.0735	0.0896
abs corrn	Semi-empirical from equivalents	Semi-empirical from equivalents	Semi-empirical from equivalents
data/restraints/param	2531 / 57 / 84	1944 / 0 / 98	10846 / 33 / 632
GOF on F^2	1.061	0.891	0.969
R_1,[b] wR_2[c] [I >2σ(I)]	0.0606, 0.1538	0.0274, 0.0685	0.0490, 0.1077
R_1,[b] wR_2[c] (all data)	0.0713, 0.1632	0.0331, 0.0723	0.0785, 0.1212
Largest diff peak and hole, e Å^{-3}	5.723 and -3.135	1.407 and -1.045	2.442 and -2.096

[a]The values are the actual formula units and weights as obtained from bulk elemental analysis.

[b]$R_1 = \Sigma||F_o| - |F_c||/\Sigma|F_o|$. [c]$wR_2 = [\Sigma w(F_o^2 - F_c^2)^2/\Sigma w(F_o^2)^2]^{1/2}$.

Table S2. Bond lengths [Å] and angles [deg] for **Na-1**.

Au-O(2)	1.95(2)	O(3)#1-Au-O(3)#2	85.5(15)
Au-O(3)#1	1.94(2)	O(3)#1-Au-O(2)	92.4(10)
Pt-O(1)	2.10(3)	O(3)#2-Au-O(2)	174.7(11)
Pt-O(2)	2.00(2)	O(2)-Au-O(2)#3	89.2(14)
O(2)#1-Pt-O(2)	92.7(10)	O(2)-Pt-O(1)#4	176.6(10)
O(2)-Pt-O(1)	86.4(10)	O(2)-Pt-O(1)#1	90.6(10)
Au-O(2)-Pt	115.6(10)	O(1)#1-Pt-O(1)	90.3(11)

Symmetry transformations used to generate equivalent atoms: #1 -y+1,x-y,z; #2 -y+1,x-y,-z+2; #3 x,y,-z+2; #4 -x+y+1,-x+1,z

Table S3. Bond lengths [Å] and angles [deg] for **Na-1a**.

Au-O(1)	1.968(4)	O(1)-Au-O(1)#1	93.4(3)
Au-O(3)	2.015(4)	O(1)-Au-O(3)#1	174.55(17)
Pt-O(1)	1.957(4)	O(1)-Au-O(3)	88.78(18)
Pt-O(2)	2.044(4)	O(3)#1-Au-O(3)	88.6(2)
O(1)-Pt-O(2)	87.98(18)	O(1)#3-Pt-O(2)	85.85(18)
O(1)-Pt-O(1)#3	94.97(16)	O(1)#4-Pt-O(2)	176.85(17)
Au-O(1)-Pt	116.4(2)	O(2)#3-Pt-O(2)	91.14(17)

Symmetry transformations used to generate equivalent atoms: #1 x,y,-z+1/2; #2 -y+1,x-y,z; #3 -x+y+1,-x+1,z; #4 -y,x-y+1,z

Table S4. Bond lengths [Å] and angles [deg] for **K-1**.

Au(1)-O(3)	1.949(9)	Pt(1)-O(10)	1.965(9)
Au(1)-O(1)	1.960(9)	Pt(1)-O(5)	1.975(8)
Au(1)-O(2)	2.002(9)	Pt(1)-O(3)	1.977(9)
Au(1)-O(4)	2.026(9)	Pt(1)-O(14)	2.049(10)
Au(2)-O(5)	1.960(8)	Pt(1)-O(13)	2.053(9)
Au(2)-O(7)	1.965(9)	Pt(1)-O(15)	2.056(9)
Au(2)-O(6)	2.012(10)	Pt(2)-O(9)	1.960(9)
Au(2)-O(8)	2.021(9)	Pt(2)-O(1)	1.966(8)
Au(3)-O(9)	1.933(9)	Pt(2)-O(7)	1.972(9)
Au(3)-O(10)	1.954(9)	Pt(2)-O(16)	2.054(9)
Au(3)-O(11)	2.011(9)	Pt(2)-O(18)	2.054(8)
Au(3)-O(12)	2.030(9)	Pt(2)-O(19)	2.063(9)
O(3)-Au(1)-O(1)	92.9(4)	O(10)-Pt(1)-O(5)	95.9(4)
O(3)-Au(1)-O(2)	174.8(4)	O(10)-Pt(1)-O(3)	95.7(4)

O(1)-Au(1)-O(2)	90.2(4)	O(5)-Pt(1)-O(3)	95.0(4)
O(3)-Au(1)-O(4)	89.2(4)	O(10)-Pt(1)-O(14)	84.2(4)
O(1)-Au(1)-O(4)	175.9(4)	O(5)-Pt(1)-O(14)	88.5(4)
O(2)-Au(1)-O(4)	87.4(4)	O(3)-Pt(1)-O(14)	176.5(4)
O(5)-Au(2)-O(7)	94.0(4)	O(10)-Pt(1)-O(13)	86.3(4)
O(5)-Au(2)-O(6)	87.6(4)	O(5)-Pt(1)-O(13)	177.0(4)
O(7)-Au(2)-O(6)	173.8(4)	O(3)-Pt(1)-O(13)	86.8(4)
O(5)-Au(2)-O(8)	174.7(4)	O(14)-Pt(1)-O(13)	89.6(4)
O(7)-Au(2)-O(8)	88.2(4)	O(10)-Pt(1)-O(15)	175.4(4)
O(6)-Au(2)-O(8)	89.7(4)	O(5)-Pt(1)-O(15)	84.3(3)
O(9)-Au(3)-O(10)	95.1(4)	O(3)-Pt(1)-O(15)	88.9(4)
O(9)-Au(3)-O(11)	85.9(4)	O(14)-Pt(1)-O(15)	91.2(4)
O(10)-Au(3)-O(11)	172.9(4)	O(13)-Pt(1)-O(15)	93.4(3)
O(9)-Au(3)-O(12)	174.8(4)	O(9)-Pt(2)-O(18)	85.5(4)
O(10)-Au(3)-O(12)	85.5(4)	O(1)-Pt(2)-O(18)	176.5(4)
O(11)-Au(3)-O(12)	92.9(4)	O(7)-Pt(2)-O(18)	87.8(4)
O(9)-Pt(2)-O(1)	94.0(4)	O(16)-Pt(2)-O(18)	89.4(3)
O(9)-Pt(2)-O(7)	95.4(4)	O(9)-Pt(2)-O(19)	176.0(3)
O(1)-Pt(2)-O(7)	95.7(4)	O(1)-Pt(2)-O(19)	89.6(4)
O(9)-Pt(2)-O(16)	86.7(4)	O(7)-Pt(2)-O(19)	85.9(4)
O(1)-Pt(2)-O(16)	87.1(3)	O(16)-Pt(2)-O(19)	91.8(4)
O(7)-Pt(2)-O(16)	176.4(4)	O(18)-Pt(2)-O(19)	90.8(4)

Table S5. Bond valence sum values for different types of μ_2-bridging oxygen atoms in **Na-1**, **Na-1a** and **K-1**. Bond valence $v_{ij} = \exp[(R_{ij}-d_{ij})/b]$ (R_{ij} = bond valence parameter; b = 0.37); bond valence sum $V_i = \Sigma_j v_{ij}$

Compound	**μ_2-O**	**BVS value**
Na-1	Au – O2 – Pt	1.433
Na-1a	Au – O1 – Pt	1.498
K-1	Au1 – O1 – Pt2	1.494
	Au1 – O3 – Pt1	1.492
	Au2 – O5 – Pt1	1.476
	Au2 – O7 – Pt2	1.470
	Au3 – O9 – Pt2	1.558
	Au3 – O10 – Pt1	1.509

Table S6. Peak assignments of the ESI-MS spectra of **Na-1** and **K-1**.

$Na[Pt_2Au_3O_6(AsO_2(CH_3)_2)_6]\cdot NaCl\cdot NaNO_3\cdot 6H_2O$ (**Na-1**)		
Formula	**Target Mass (amu)**	**Measured Mass (amu)**
$[Pt_2Au_3O_6(AsO_2(CH_3)_2)_6]^-$	1898.9887	1898.7804
$[Na_2Pt_2Au_3O_6(AsO_2(CH_3)_2)_6]^+$	1944.9682	1944.4715
$[Na_3Pt_2Au_3O_6(AsO_2(CH_3)_2)_6]^{2+}$	983.979	983.7274
$K[Pt_2Au_3O_6(AsO_2(CH_3)_2)_6]\cdot KCl\cdot KAsO_2(CH_3)_2\cdot 18H_2O$ (**K-1**)		
Formula	**Target Mass (amu)**	**Measured Mass (amu)**
$[Pt_2Au_3O_6(AsO_2(CH_3)_2)_6]^-$	1898.9887	1898.8694
$[K_2Pt_2Au_3O_6(AsO_2(CH_3)_2)_6]^+$	1977.1853	1976.4124
$[K_3Pt_2Au_3O_6(AsO_2(CH_3)_2)_6]^{2+}$	1008.1418	1007.6855

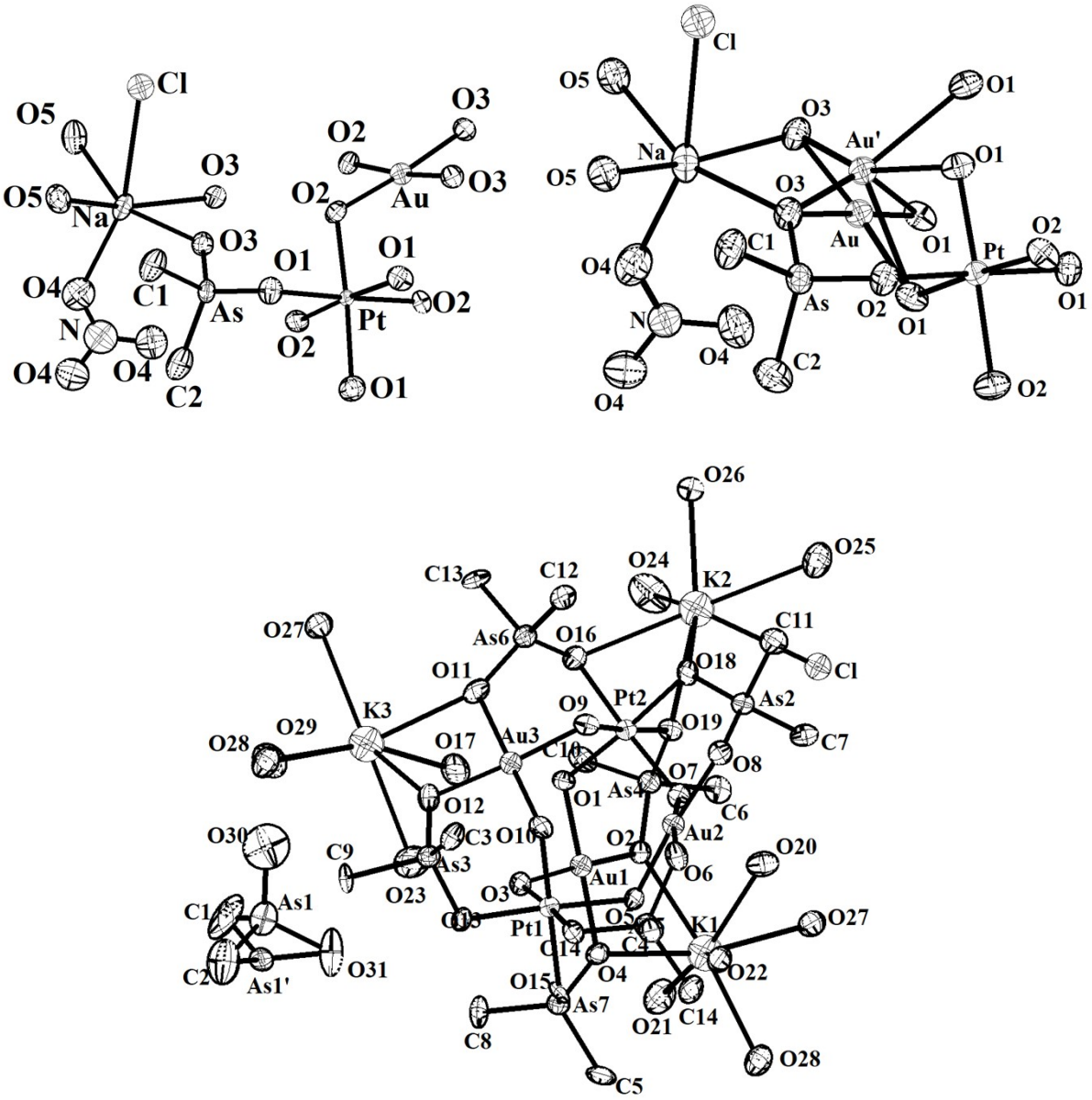

Figure S1. The symmetry unit of solid-state interaction of polyanion **1** with Na^+ counter cations in **Na-1** (top left) and **Na-1a** (top right), as well as K^+ counter cations in **K-1** (bottom), respectively (50% probability ellipsoids). Hydrogen atoms omitted for clarity.

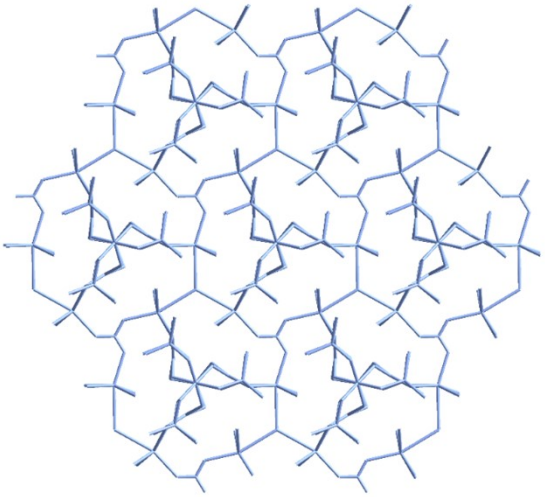

Figure S2. Solid state structure of **Na-1** highlighting the supramolecular 2D layered plane.

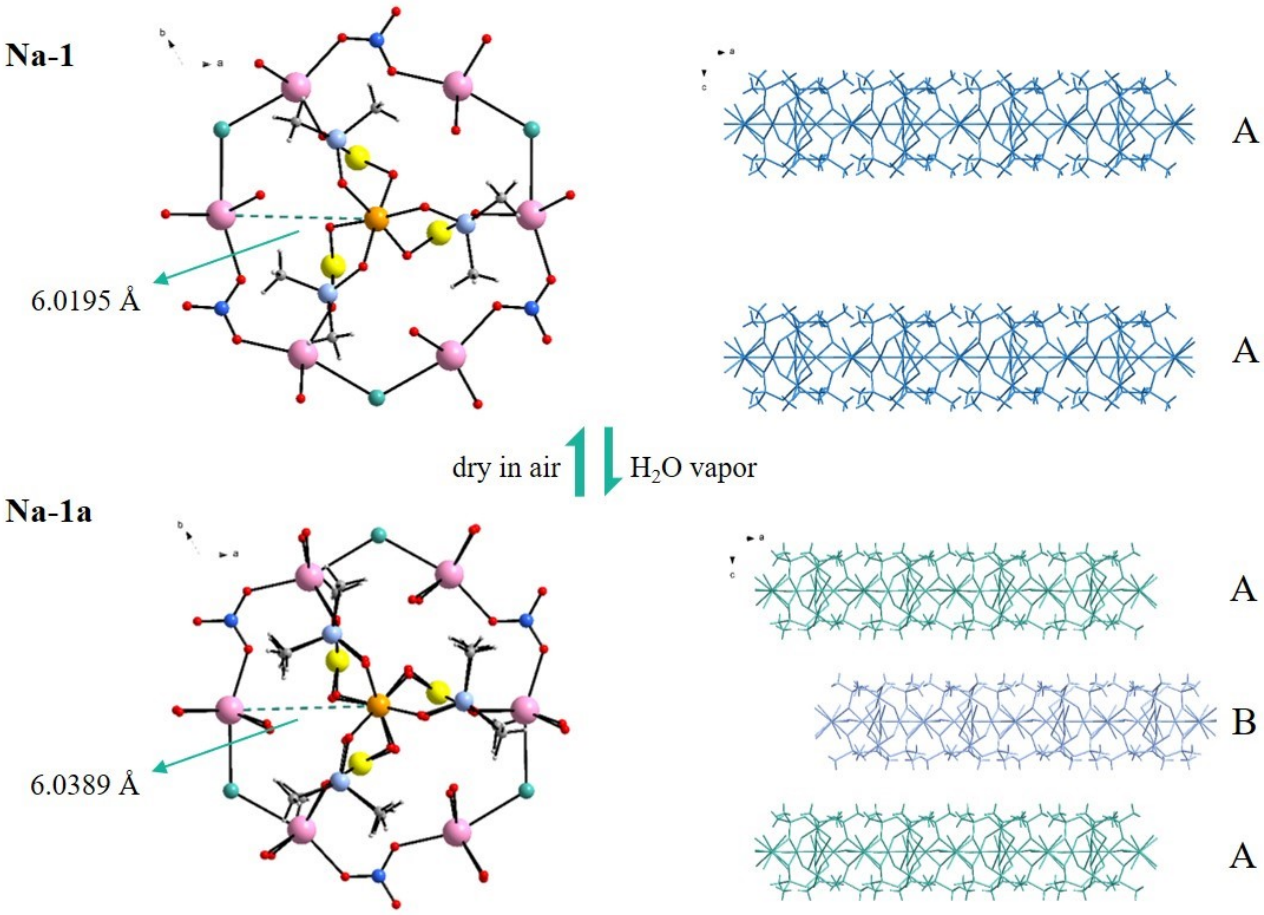

Figure S3. The fully reversible SCSC transition of **Na-1** to **Na-1a**. Left: ball-and-stick representation; right: packing diagrams for **Na-1** (AA mode) and **Na-1a** (AB mode). Color code: Au yellow, Pt orange, O red, C grey, N blue, As light blue, Cl light green, Na pink, H light grey.

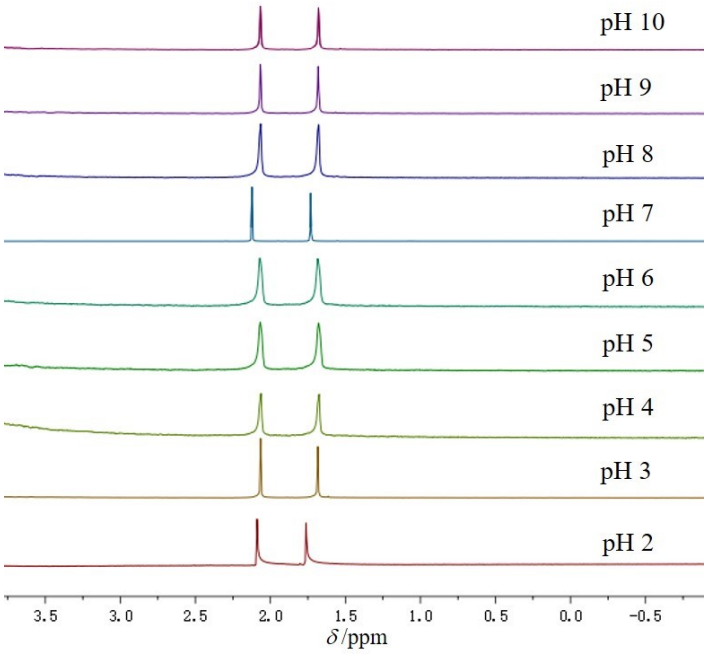

Figure S4. pH-dependent ^{1}H NMR spectra (D_2O/H_2O) of **Na-1**.

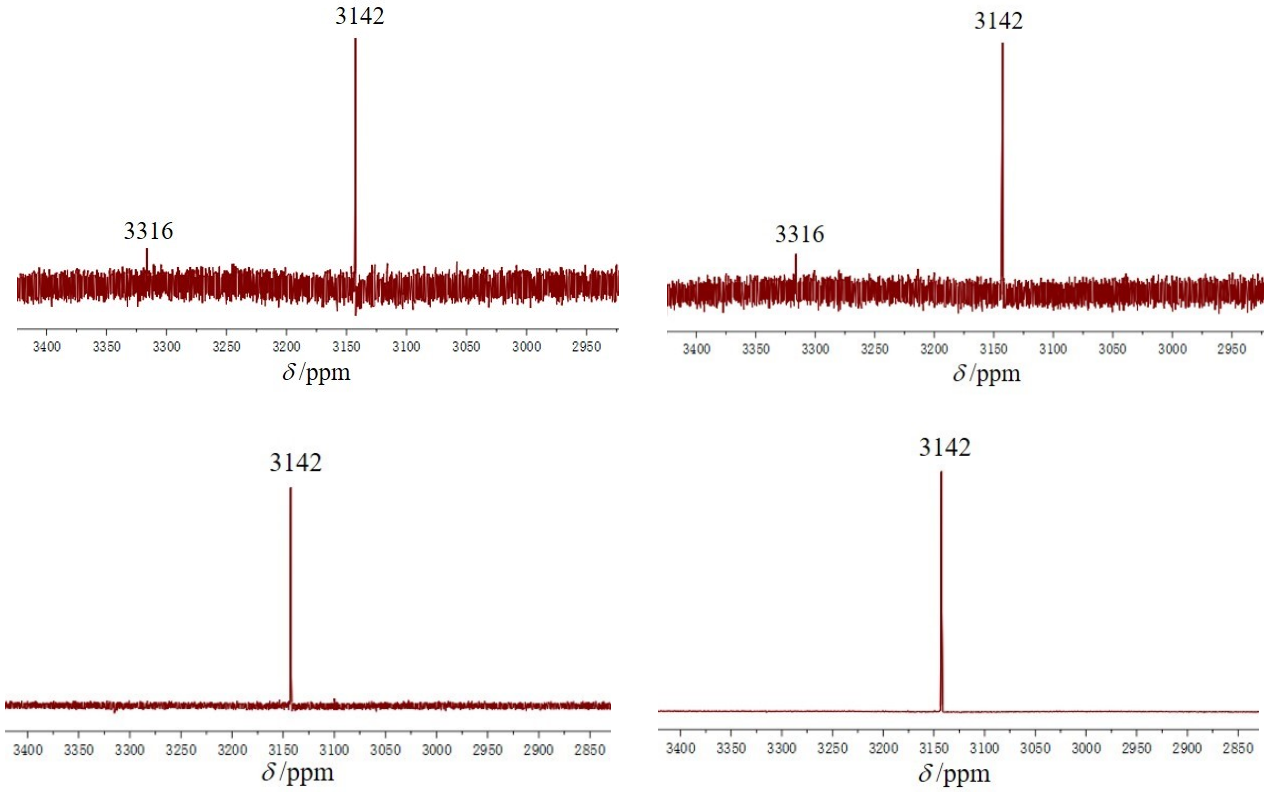

Figure S5. ^{195}Pt NMR spectra of fresh synthesis solutions of **Na-1** after stirring at room temperature for 10 min (top left, 4510 scans) and for 40 min (top right, 3018 scans), as well as at 40 ºC for 30 min (bottom left, 3052 scans) and the same solution after a longer measurement time (bottom right, 126693 scans).

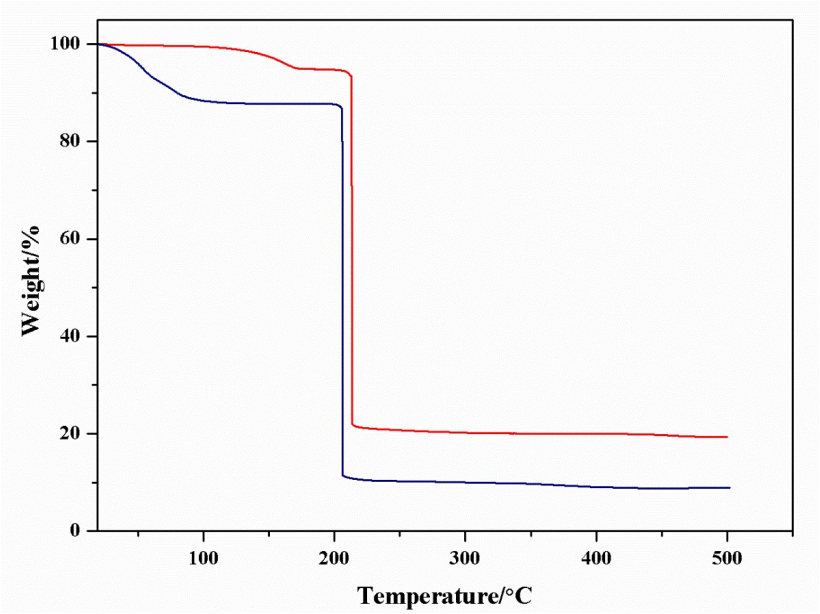

Figure S6. Thermograms of **Na-1** (red) and **K-1** (blue) from room temperature to 500 °C under N_2 atmosphere.

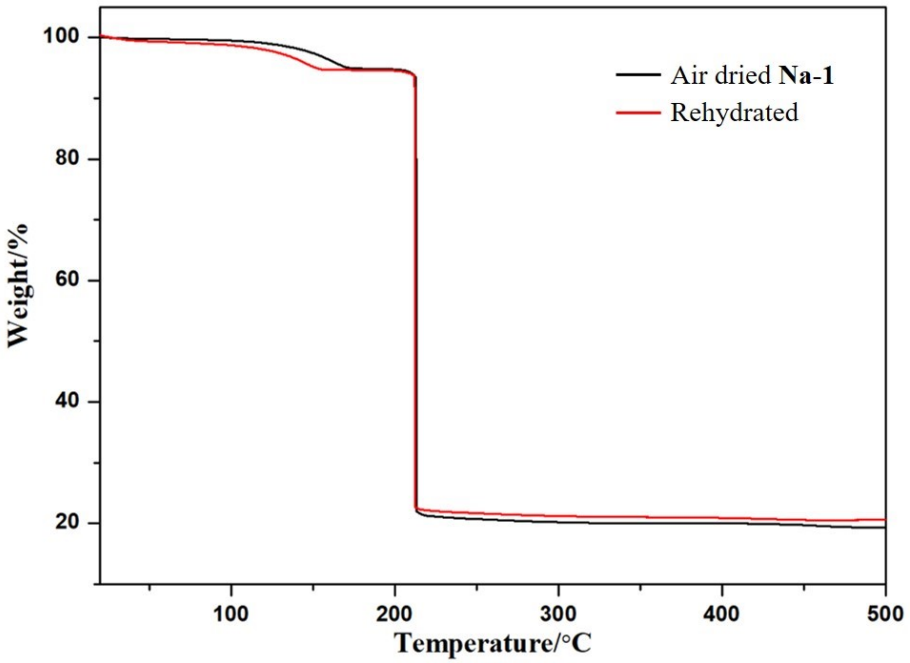

Figure S7. Thermograms of air-dried and partially rehydrated (several hours) **Na-1** from room temperature to 500 °C under N_2 atmosphere. Complete rehydration of the bulk material **Na-1** results in partial dissolution.

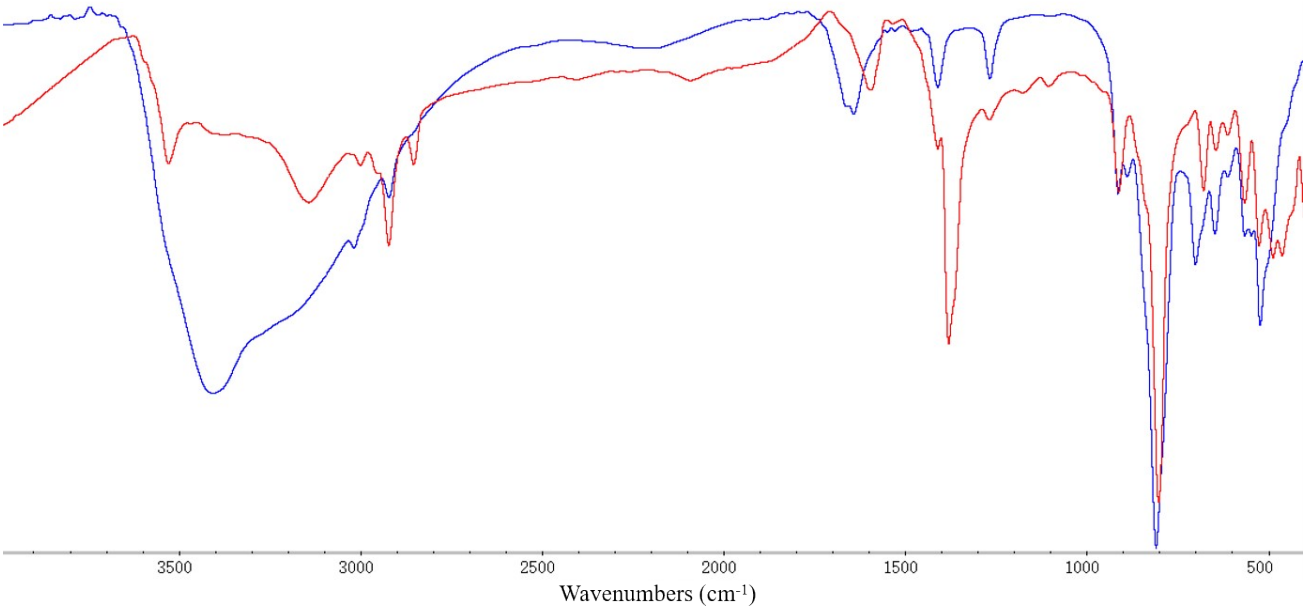

Figure S8. FT-IR spectra of **Na-1** (red) and **K-1** (blue) from 400–4000 cm^{-1} on KBr pellets.

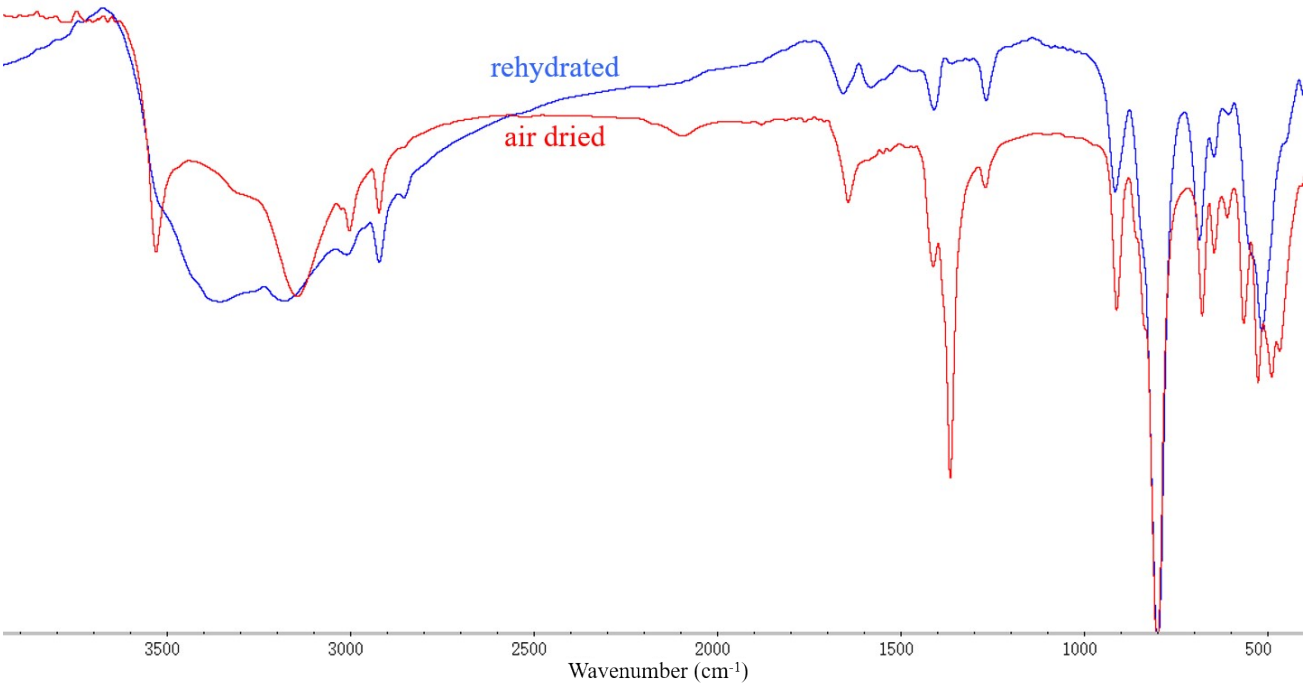

Figure S9. FT-IR spectra of air-dried and rehydrated **Na-1** from 400–4000 cm^{-1} on KBr pellets.

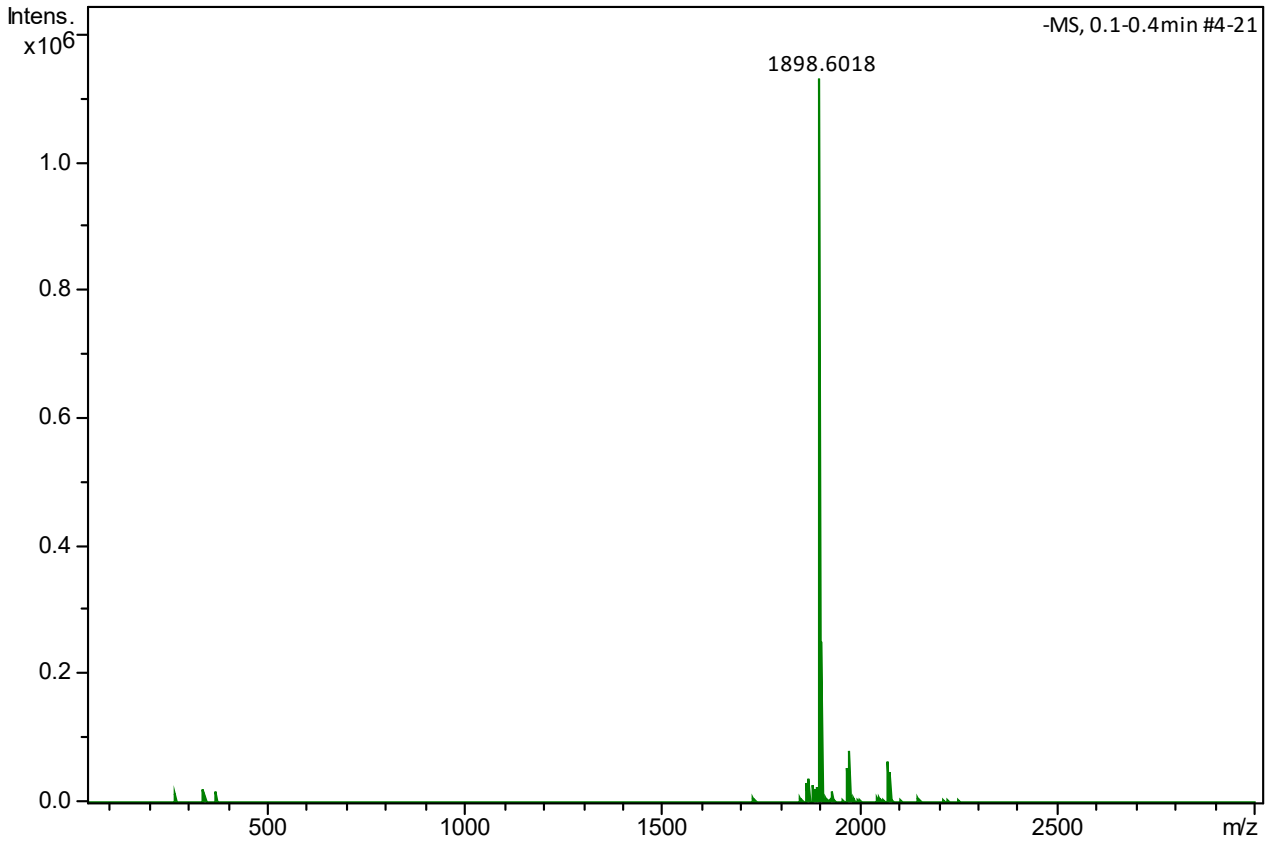

Figure S10. ESI-MS spectrum (full scan) for aqueous solutions of **Na-1** in the negative-ion mode (identical result for **K-1**).

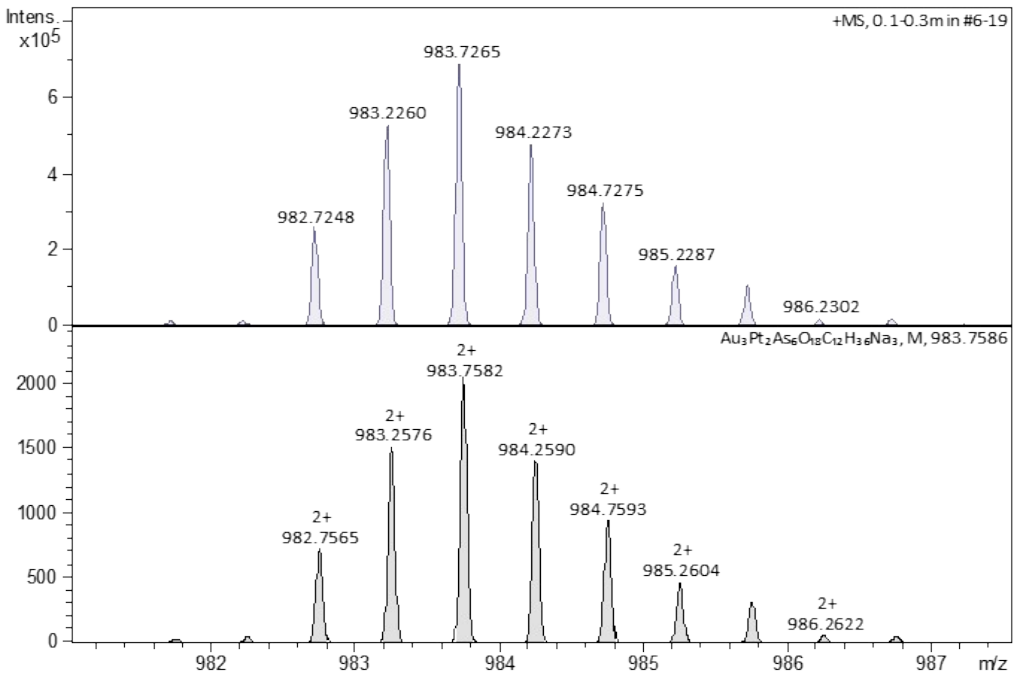

Figure S11. Simulated ESI-MS spectrum of **Na-1** in positive-ion mode (bottom) and experimental ESI-MS spectrum (top) of the doubly-charged $[Na_3Pt_2Au_3O_6(AsO_2(CH_3)_2)_6]^{2+}$ ion (expanded view).

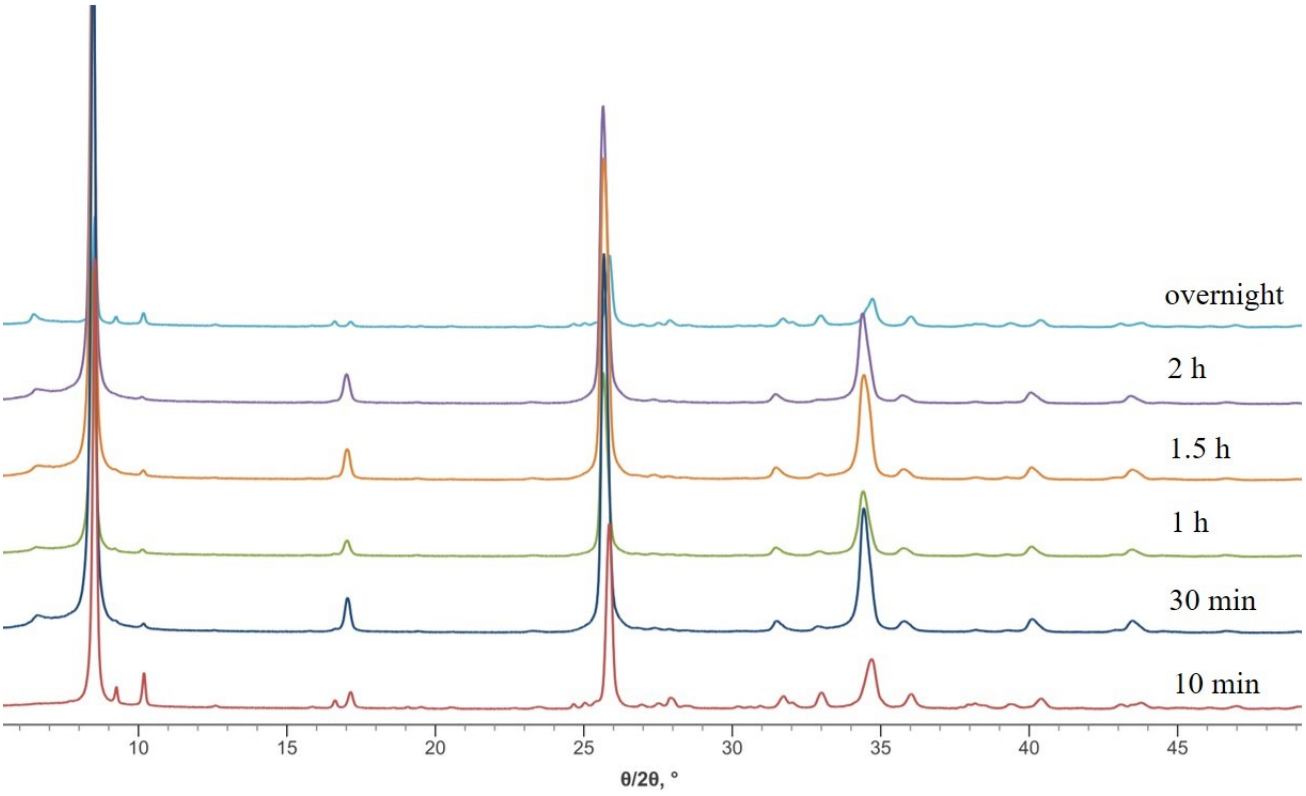

Figure S12. PXRD patterns for **Na-1** in the presence of water vapor for different periods of time at RT.

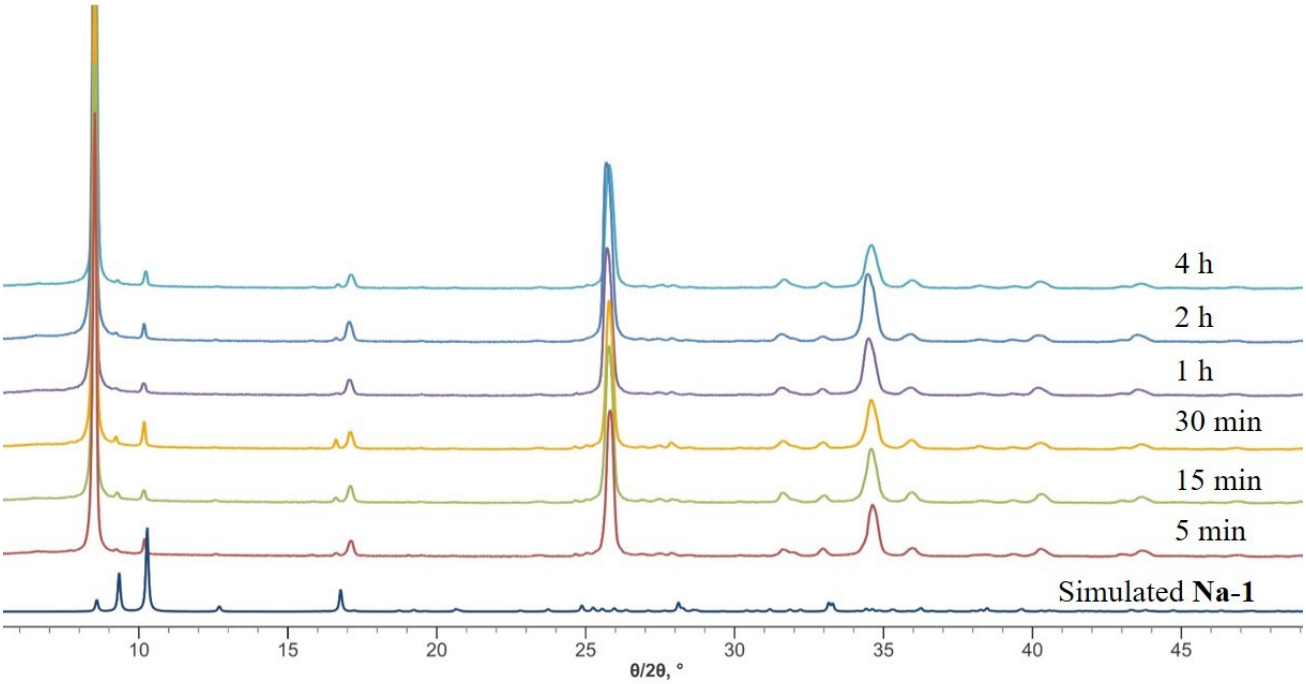

Figure S13. Time-dependent PXRD spectra of **Na-1** under blue light irradiation.

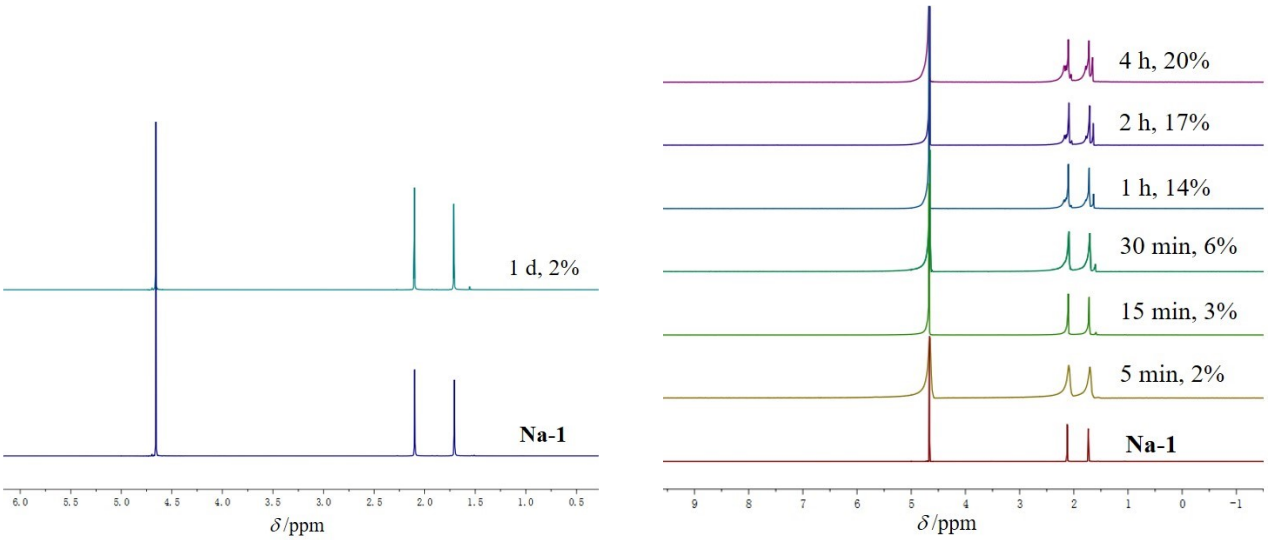

Figure S14. Time-dependent ^{1}H NMR spectra of **Na-1** without (left) and with (right) blue light irradiation.